

Phonon spectra and heat capacity of $\text{Li}_2\text{B}_4\text{O}_7$ and LiB_3O_5 crystals

V.V. Maslyuk^{1,a}, T. Bredow², and H. Pfnür¹

¹ Institut für Festkörperphysik, Universität Hannover, Appelstr. 2, 30167 Hannover, Germany

² Theoretische Chemie, Universität Hannover, Am Kleinen Felde 30, 30167 Hannover, Germany

Received 15 July 2004

Published online 18 January 2005 – © EDP Sciences, Società Italiana di Fisica, Springer-Verlag 2004

Abstract. The results of calculations of the phonon dispersion, the vibrational density of states and the heat capacity of lithium tetraborate and lithium triborate crystals are presented. They are obtained in the framework of a potential model that takes into account the non-equivalence of boron atoms in different structural positions (BO_3 and BO_4 units). A symmetry analysis of the phonon modes at Γ point was performed, and calculated frequencies are compared to experimental spectra. Analysis of Li contributions to the vibrational density of states reveals that the Li-O bonds in both crystals are relatively weak. This is in line with the experimentally observed high mobility of lithium ions at high temperatures. A good agreement between calculated and measured heat capacities from the literature was obtained.

PACS. 61.50.Ah Theory of crystal structure, crystal symmetry; calculations and modeling – 12.39.Pn Potential models – 65.40.Ba Heat capacity – 63.20.Dj Phonon states and bands, normal modes, and phonon dispersion

1 Introduction

Due to their interesting characteristics (e.g., a negative thermal expansion coefficient along the (001) direction, and transparency in the UV-region) lithium tetraborate (LTB) and lithium triborate (LBO) crystals are used as materials for wave-guides [1], the 2th–5th YAG:Nd single crystal laser harmonics generation [2–7] and thermoluminescent dosimetry [8–10].

Despite the large number of experimental and theoretical studies of LTB and LBO crystals, the mechanism of lithium ion dynamics as well as the behavior of the phonon subsystem within a wide temperature range is still not understood. The complexity of the crystal structures of $\text{Li}_2\text{B}_4\text{O}_7$ (space group $I4_1cd$, 52 atoms in the primitive cell [11]) and of LiB_3O_5 (space group $Pna2$, 36 atoms in the primitive cell [12]) makes it difficult to apply *ab initio* methods, in particular for the calculation of dynamic properties. Thus, an alternative approach was to find an appropriate classical potential model that can be used for molecular dynamics calculations in order to simulate the phonon spectra, the heat capacity, and also allows to investigate the migration of Li atoms.

This has been achieved in a recent study [13] where we proposed a potential model for single crystals of the $\text{Li}_2\text{O}-\text{B}_2\text{O}_3$ system. In this approach two types of boron atoms are distinguished with different hybridization states, namely sp^2 (in BO_3), and sp^3 (in BO_4). The two

types of boron, B^1 and B^2 , are described with the same mass but with different effective charges and parameters for the B-O interaction potentials.

Based on this model, we present results for the phonon dispersion, the vibrational density of states (VDOS) and the temperature dependence of the heat capacity for both $\text{Li}_2\text{B}_4\text{O}_7$ and LiB_3O_5 crystals. The calculated results are compared with available experimental data from the literature.

2 Calculation procedure

Our potential model is based on two- and three-body interactions. The two-body interactions were treated by means of the classical Buckingham potential and a Coulomb term [14]

$$U_{ij} = b_{ij} \exp\left(-\frac{r_{ij}}{\rho_{ij}}\right) + \frac{q_i q_j e^2}{r_{ij}} \quad (1)$$

where r_{ij} is the bond length between ions i and j ; $q_i e$ is the charge of ion i . The Coulombic component was calculated under periodic boundary conditions using the Ewald summation [15].

A harmonic potential [14] was chosen to describe three-body interactions:

$$U_{ijk} = \frac{1}{2} A_{ijk} (\Theta_{ijk} - \Theta_0)^2, \quad (2)$$

where A_{ijk} are constants determining the strength of the interaction, Θ_{ijk} is the angle between i - j and j - k bonds

^a e-mail: maslyuk@mail.ru

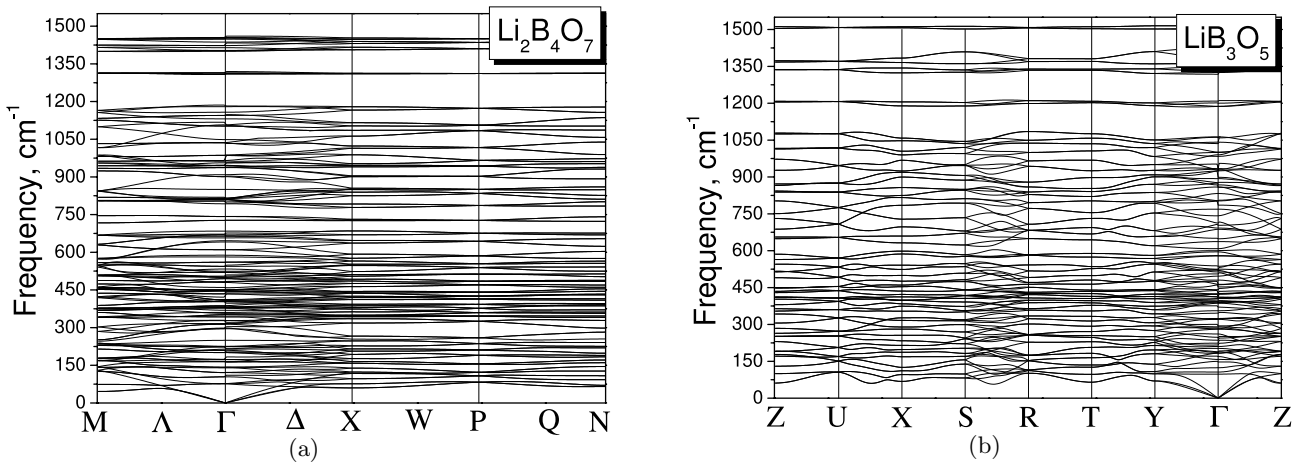


Fig. 1. The calculated phonon dispersion of LTB (a) and LBO (b) crystals.

and Θ_0 is the equilibrium angle. The values of the parameters that appear in equations (1–2) have been optimized for $\text{Li}_2\text{B}_4\text{O}_7$ [13]. The calculations were performed using the GULP code [14].

First we investigated the phonon dispersion within the harmonic approximation by solving the standard eigen-problem of the secular equation resulting from the dynamical matrix. In the next step the vibrational density of states of LTB and LBO was obtained. For testing our potential model we calculated VDOS in two ways. In the harmonic approach, the VDOS is calculated as the sum of all vibrational states in the Brillouin zone using a k -point grid of $20 \times 20 \times 20$. The second approach is based on linear response theory, where the phonon density of states $g(\nu)$ can be obtained as Fourier transform of the velocity autocorrelation function [16]:

$$g(\nu) = \sum_{i=1}^N \int_0^{\infty} \frac{\langle V_i(0)V_i(t) \rangle}{\langle V_i(0)^2 \rangle} \cos(2\pi\nu t) dt, \quad (3)$$

where $V_i(t)$ is the velocity of the i th atom computed at each time step (every 1 fs) using the Verlet algorithm and N is the total number of lithium, boron and oxygen ions in the simulation box. The molecular dynamics calculation was performed with a NPT-ensemble in conjunction with the Nosé-Hoover [17] thermostat and the Parrinello-Rahman [18] barostat. The computation box contained 832 atoms ($2 \times 2 \times 2$ supercell) for $\text{Li}_2\text{B}_4\text{O}_7$ and 432 atoms ($2 \times 2 \times 3$ supercell) for LiB_3O_5 . The system was allowed to evolve for 50 ps, the first 35 ps of which were used for equilibration and were not included in the results. The calculation was performed at a relatively low temperature of 25 K because the Fourier transform of the velocity autocorrelation function can be used only within the validity range of the harmonic approximation [16].

In both cases $g(\nu)$ was normalized according to

$$\int_0^{\infty} g(\nu) d\nu = 1. \quad (4)$$

The projection of $g(\nu)$ onto atomic species (PVDOS) was calculated from equation (3) where the summation was only performed for the individual ions Li, B¹, B² and O.

The phonon specific heat of the LTB and LBO crystals at constant volume was obtained from the corresponding VDOS using the following relation [19]

$$C_v = k_B \int_0^{\nu_{max}} g(\nu) \left(\frac{h\nu}{k_B T} \right) \frac{\exp(h\nu/k_B T)}{(1 - \exp(h\nu/k_B T))^2} d\nu, \quad (5)$$

where k_B is the Boltzmann factor, ν_{max} is the highest frequency recorded in the $g(\nu)$ spectrum and T the temperature.

3 Results and discussion

3.1 Phonon dispersion

Using group theory the following decomposition of the normal vibration modes of $\text{Li}_2\text{B}_4\text{O}_7$ [20] and LiB_3O_5 [21] was obtained:

$$\text{LTB: } \Gamma = 19A_1 + 19A_2 + 19B_1 + 19B_2 + 40E$$

$$\text{LBO: } \Gamma = 29A_1 + 27A_2 + 26B_1 + 26B_2,$$

where one A_1 and one E mode for LTB and three A_1 modes for LBO are acoustic.

The vibrational spectra of the $\text{Li}_2\text{B}_4\text{O}_7$ and LiB_3O_5 crystals were studied experimentally by Raman and IR spectroscopy methods [20–26]. The superposition of experimental spectra for $\text{Li}_2\text{B}_4\text{O}_7$ [20, 22–24] exhibit a larger number of A_1 , B_1 , and B_2 modes than theory predicts. This is partly due to technical difficulties of the measurements that lead to incomplete spectra. For instance, A_2 modes are completely unknown and only 34 E modes have been observed for the LTB crystal instead of 40 as predicted by theory. This can be explained by the complexity of the spectra and by the small intensity of the majority of modes. It is also possible that local defect vibrations and overtones are present.

The phonon dispersion was calculated along the way that contains the highest number of high-symmetry points of the Brillouin zone [27], namely for LTB: $M \rightarrow \Gamma \rightarrow X \rightarrow P \rightarrow N$, and for LBO: $Z \rightarrow U \rightarrow X \rightarrow S \rightarrow R \rightarrow T \rightarrow Y \rightarrow \Gamma \rightarrow Z$. The results of our calculations are shown in Figure 1.

Table 1. The A_1 modes of $\text{Li}_2\text{B}_4\text{O}_7$ phonon spectra (cm^{-1}). Lines that were described as diffuse in the literature are marked by ‘d’.

N	Calculated data	Exper. [20]		Exper. [23]			Exper. [24]	
		TO	LO	TO (Raman)	TO (IR)	LO (Raman)	LO (IR)	TO
1	0.0	0.0						
2	165.2	153	159	157		164		158
3	205.2	196	171	194		205		197 222
4	275.7	262	272	255	255	271	278	256
5	321.6	299	300	295	303	296	304	298
6	356.0	351	355	338	347	362	367	351
7	376.9				382		388.5	
8	442.2	425	427		426		427	
9	457.5	495	495	491	489	479	489.5	493
10	517.3	508	509	507	509.5	508	513.5	507 531 562
11	588.5							
12	665.3			688	689	694	698.5	
		724	725	722	719	723	719.5	725
13	799.9	781	784	778	779	788	788.5	781
14	806.8	849	849					
15	939.4							
16	991.2	980	975	974	980.5			980
		1034	1034	1027	1038	1031	1038	1034 1060
17	1179.6	1166	1167	1159	1154.5	1164	1170.5	1166
		1300	1302	1296	1276		1280	
		1350d	1350d					
18	1403.3							
19	1453.8			1400	1390		1436	
		1550d	1550d					

Figure 1 illustrates the complexity of the lithium tetraborate and triborate phonon spectra that are due to the complexity of their primitive cells. 156 (105) vibrational modes for LTB (LBO) were found. Our calculation shows that some band gaps are present. They separate the high-energy bands from inner rigid vibrations of BO_3 and BO_4 complexes.

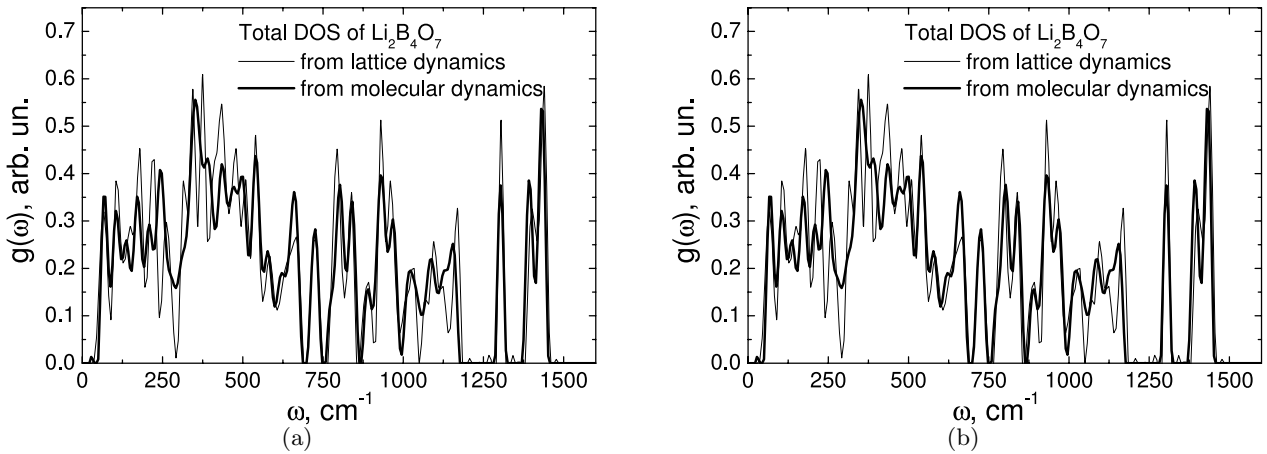
A symmetry analysis was performed by comparing the basis functions of the irreducible representations with the eigenvectors of each vibrational mode at the Γ point. A_1 symmetry modes at the Γ point and their comparison with the experimental data for $\text{Li}_2\text{B}_4\text{O}_7$ and LiB_3O_5 are given in Tables 1 and 2. For brevity we have restricted the comparison of theory and experiment to the A_1 representation. The agreement for the other symmetry modes is similar.

As can be seen from Tables 1 and 2, good agreement between most calculated and experimental vibrational modes was obtained. It should be noticed here

that frequencies were not used as input data to determine the potential model. Some calculated frequencies, however, are shifted with respect to the experimental results. This can be explained by the underlying harmonic approximation, while most experimental results were obtained at room temperature where anharmonic contributions are non-negligible. The maximal difference between calculated and measured frequencies is 50 cm^{-1} for the line at 1501 cm^{-1} of the LiB_3O_5 crystal. In general the average deviation from experimental results is about 17 cm^{-1} for LiB_3O_5 and 18 cm^{-1} for $\text{Li}_2\text{B}_4\text{O}_7$. This is in the range of empirical calculations [28]. In both tables there are a few other modes that are present in experiment and absent in the calculated spectra. The analysis of experimental spectra [20–23] show that the intensities of these lines are small. Thus it is possible that the additional modes in the experimental spectra are local defect vibrations, polarons, or overtones as suggested in references [20] and [24]. It is also possible that isotope effects play a role.

Table 2. The A_1 modes of LiB_3O_5 phonon spectra (cm^{-1}).

N	Calculated data	Exper. [21]	N	Calculated data	Exper. [21]	N	Calculated data	Exper. [21]
1	124	136.7	11	441	445	20	924	918.7
2	158	164	12	505	485			955
3	186	195	13	523	552.3			991.7
4	216	222	14	600	607.7	21	1036	1024
5	224		15	637	648.7	22	1042	1077
6	321				669	23	1209	
7	346	343	16	712	737.5	24	1318	1343.3
8	396		17	742	763.3	25	1363	1361
9	403		18	803				1388.5
10	413	423.3	19	877	899.6	26	1501	1553

**Fig. 2.** Phonon DOS of LiB_3O_5 crystals: (a) total VDOS; (b) projection of the total VDOS onto atomic species.

The natural isotope distribution of Li and B atoms are ^6Li (7.4%) and ^7Li (92.6%), and ^{10}B (20%) and ^{11}B (80%), respectively. Therefore contributions from ^6Li and ^{10}B are not negligible. They are not included in our calculations.

3.2 The vibrational VDOS and its projections

In Figures 2 and 3 the calculated VDOS of $\text{Li}_2\text{B}_4\text{O}_7$ and LiB_3O_5 obtained by two different simulation methods are shown. Good agreement between the harmonic approach (from lattice dynamics) and the Fourier transform of the velocity autocorrelation function (from molecular dynamics) is obtained for the total VDOS of LTB and LBO crystals (Figs. 2a, 3a). These spectra are a first investigation of VDOS for the lithium anhydrous borate crystals. One can see that the projected DOS of $\text{Li}_2\text{B}_4\text{O}_7$ and LiB_3O_5 show similar behavior.

The oxygen projections of the phonon density of states show that the oxygen atoms are involved in all modes. They have the highest contribution in the total VDOS (Figs. 3b, 2b) which was expected from the stoichiometry of the crystals. Note that for both LTB and LBO

the lithium PVDOS is restricted to the low-frequency region up to 600 cm^{-1} giving evidence that the Li-O bonds are weak. Therefore, as for the similar Li-containing systems [29,30], lithium can easily diffuse in these crystals. In the region up to 600 cm^{-1} also contributions of the B^1 and B^2 PVDOS are present but the intensities are three times smaller than for lithium.

The medium-frequency region (from 600 cm^{-1} to 1200 cm^{-1}) mainly consists of projections of contributions from B^i and O atoms. The B^1 PVDOS dominates from 600 cm^{-1} to 780 cm^{-1} , and the B^2 PVDOS from 780 cm^{-1} to 1200 cm^{-1} . The high-frequency region is dominated by local vibrations of BO_3 and BO_4 complexes, with larger contributions from the B^1 -O bonds than from B^2 -O bonds.

3.3 Heat capacity of $\text{Li}_2\text{B}_4\text{O}_7$ and LiB_3O_5

The calculated specific heat capacities for both crystals (using Eq. (5)) are shown in Figure 4. Only a small difference between calculated and experimental specific heat capacity [31] is present for LTB crystals above 200 K. For

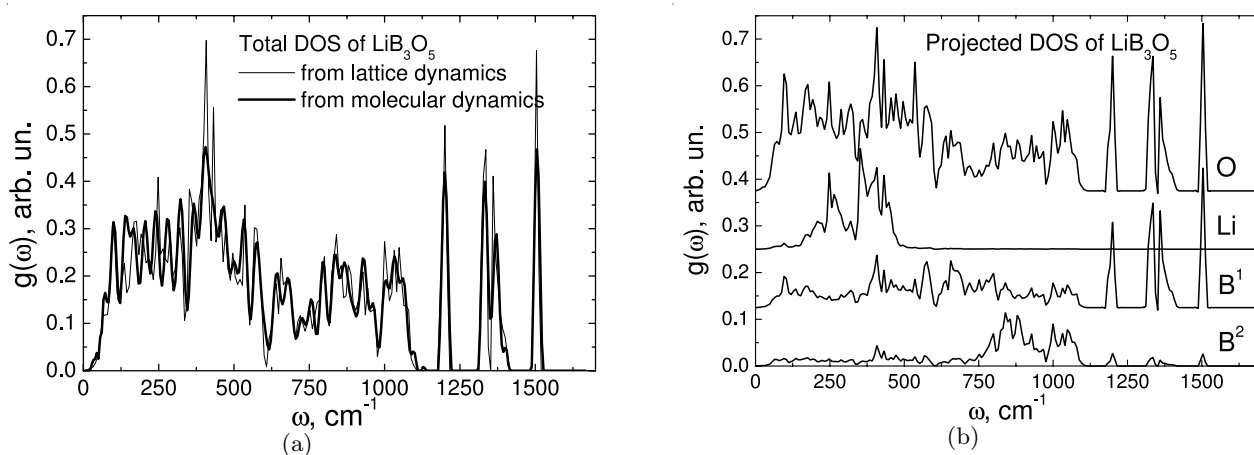


Fig. 3. Phonon DOS of $\text{Li}_2\text{B}_4\text{O}_7$ crystals: (a) total VDOS; (b) projection of the total VDOS onto atomic species.

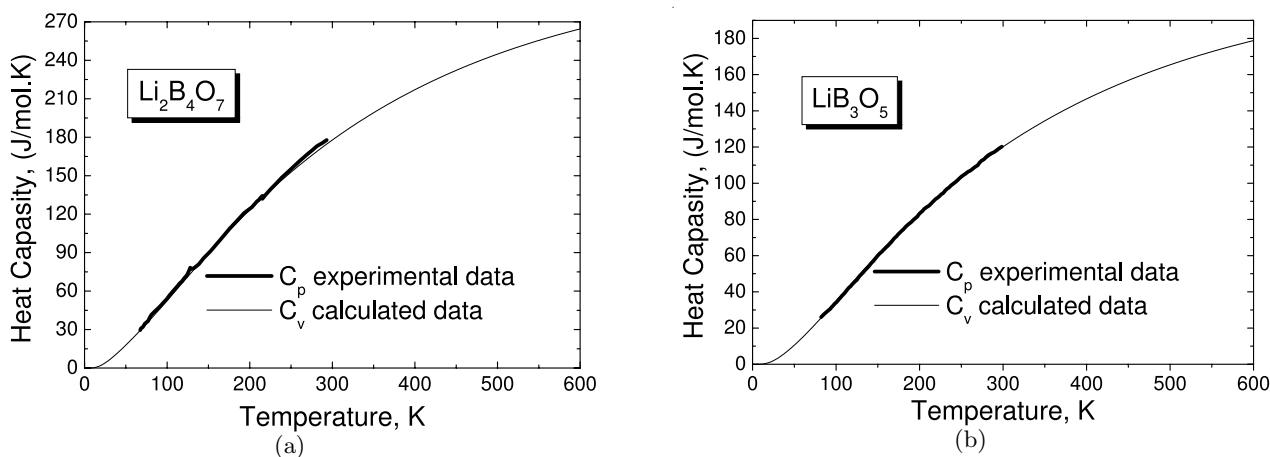


Fig. 4. The specific heat capacity of LTB (a) and LBO (b) crystals.

LBO crystal we have excellent agreement between experimental [32] and calculated results.

The experimentally measured heat capacity at constant pressure, C_p , is related to C_v by the thermodynamic relation [19]:

$$C_p(T) = C_v(T) + \alpha^2(T) \cdot T \cdot B(T) \cdot V(T), \quad (6)$$

where $\alpha^2(T)$ is the thermal expansion coefficient, $B(T)$ is the bulk modulus and $V(T)$ is the molar volume at a given temperature. Taking into account that tetraborate and triborate of lithium have small changes of lattice parameters with temperature and the lattice vector c has an abnormal temperature behaviour [26,33] we can assume that $B(T)$ is small and changes a little with temperature for both crystals.

4 Summary

In the present study, a classical approach was used to describe the phonon properties of the $\text{Li}_2\text{B}_4\text{O}_7$ and LiB_3O_5 crystals. The investigation was based on our previous work where the potential model for single crystals of

the $\text{Li}_2\text{O}-\text{B}_2\text{O}_3$ system was created. The phonon dispersion, vibrational density of state (total and its projections on atomic species) and the specific heat capacity have been calculated. The analysis of VDOS projections show that BO interactions in BO_3 are stronger than in BO_4 . The weakness of the Li-O interaction is in accord with the experimentally observed high mobility of Li ions. Good agreement of the calculated heat capacity with available experimental data has been obtained for both systems.

This work was supported by the Deutscher Akademischer Austauschdienst. The author (V.V. Maslyuk) is grateful to Prof. V.M. Rizak for suggesting the subject of studies, to Dr. V.M. Holovey, Dr. K.Z. Rushchanskii for valuable comments.

References

1. B. Wu, F. Xie, C.C.D. Deng, Z. Xu, *Opt. Commun.* **88**, 451 (1992)
2. B.S.R. Sastry, F.A. Hummel, *J. Am. Ceram. Soc.* **41**, 7 (1958)

3. B.S.R. Sastry, F.A. Hummel, *J. Am. Ceram. Soc.* **42**, 216 (1959)
4. V.I. Aver'yanov, A.E. Kalmykov, *Glass Phys. Chemistry* **16**, 492 (1990)
5. J. Huang, Y. Shen, *Appl. Phys. Lett.* **15**, 1579 (1991)
6. Mao Hongnei, *Appl. Phys. Lett.* **61**, 1148 (1992)
7. T. Ukachi, R.J. Lane, *J. Opt. Soc. Amer. B.* **9**, 1128 (1992)
8. C. Furetta, P.S. Weng, *Operation Thermoluminescent dosimetry* (World Scientific, London, 1998)
9. K. Mahesh, P.S. Weng, C. Furetta, *Thermoluminescence in solids and its applications* (Nuclear Technology Publishing, Ashford, 1989)
10. E.F. Dolzhenkova, V.N. Baumer, A.V. Tolmachev, B.M. Hunda, P.P. Puga, *6th Intern. Confer. on Inorganic Scintillators and their Applications* (Book of Abstracts, Chamonix, France, 2001), p. 210
11. S.F. Radaev, L.A. Muradyan, L.F. Malakhova, Y.A. Burak, V.I. Simonov, *Kristallografiya* **34**, 1400 (1989)
12. S.F. Radaev, B.A. Maximov, V.I. Simonov, B.V. Andreev, V.A. D'yakov, *Acta Crystallogr. B* **48**, 154 (1992)
13. V.V. Maslyuk, T. Bredow, H. Pfnür, *Eur. Phys. J. B* **41**, 281 (2004)
14. J.D. Gale, *Phil. Mag. B* **73**, 3 (1996); J.D. Gale, *J. Chem. Soc. Faraday Trans.* **93**, 629 (1997); J.D. Gale, A.L. Rohl, *Molec. Simulation* **29**, 291 (2003)
15. P.P. Ewald, *Ann. Phys.* **64**, 253 (1921)
16. P.M. Allen, D.J. Tildesley, *Computer Simulation of Liquids* (Clarendon Press, Oxford, 1989)
17. W.G. Hoover, *Phys. Rev. A* **31**, 1695 (1985)
18. M. Parrinello, A. Rahman, *J. Appl. Phys.* **52**, 7182 (1981)
19. D.C. Wallace, *Thermodynamics of Crystals* (Wiley, New York, 1976)
20. G.L. Raul, W. Taylor, *J. Phys. C: Solid State Phys.* **15**, 1753 (1982)
21. H.R. Xia, L.X. Li, H. Yu et al., *J. Mater. Res.* **16**, 3464 (2001)
22. N.D. Zhigadlo, M. Zhang, E.K.H. Salje, *J. Phys.: Condens. Matter* **13**, 6551 (2001)
23. A.V. Vdovin, V.N. Moiseenko, V.S. Gorelik, Ya.V. Burak, *Phys. Sol. State* **43**, 1648 (2001)
24. Ya.V. Burak, I.B. Trach, V.T. Adamiv, I.M. Teslyuk, *Ukrain. Phys. J.* **47**, 923 (2002)
25. V.N. Moiseenko, A.V. Vdovin, Ya.V. Burak, *Optic and Spectroscopy* **81**, 620 (1996)
26. H.R. Xia, S.M. Dong, Q.M. Lu et al., *J. Raman Spect.* **35**, 148 (2004)
27. O.V. Kovalev, *Representations of the Crystallographic Space Groups: Irreducible Representations, Induced Representations, and Corepresentations* (Gordon and Breach, Philadelphia, 1993)
28. J. Kučera, P. Nachtigall, *Collect. Czech. Chem. Commun.* **68**, 1848 (2003)
29. H. Lammert, M. Kunow, A. Heuer, *Phys. Rev. Lett.* **90**, 215901 (2003)
30. A. Heuer, M. Kunow, M. Vogel, R.D. Banhatti, *Phys. Chem. Chem. Phys.* **4**, 3185 (2002)
31. N.P. Techanovich, A.U. Sheleg, Ya.V. Burak, *Phys. Sol. State* **32**, 2513 (1990)
32. A.U. Sheleg, T.I. Dekola, N.P. Tekhanovich, A.M. Luginets, *Phys. Sol. State* **39**, 624 (1997)
33. V.V. Zaretskiĭ, Ya.V. Burak, *Phys. Sol. State* **31**, 960 (1989)